

## An ohmic nanocontact to GaAs

Takhee Lee

Department of Physics, Purdue University, West Lafayette, Indiana 47907

Jia Liu

School of Chemical Engineering, Purdue University, West Lafayette, Indiana 47907

D. B. Janes and V. R. Kolagunta<sup>a)</sup>

School of Electrical and Computer Engineering, Purdue University, West Lafayette, Indiana 47907

J. Dicke, R. P. Andres, and J. Lauterbach

School of Chemical Engineering, Purdue University, West Lafayette, Indiana 47907

M. R. Melloch, D. McInturff, and J. M. Woodall

School of Electrical and Computer Engineering and NSF MRSEC for Technology Enabling Heterostructure Materials, Purdue University, West Lafayette, Indiana 47907

R. Reifenger<sup>b)</sup>

Department of Physics, Purdue University, West Lafayette, Indiana 47907

(Received 28 January 1999; accepted for publication 17 March 1999)

The formation and characterization of nanometer-size, ohmic contacts to *n*-type GaAs substrates are described. The nanocontacts are formed between a single-crystalline, nanometer-size Au cluster and a GaAs structure capped with layer of low-temperature-grown GaAs (LTG:GaAs). An organic monolayer of xylyl dithiol (*p*-xylene- $\alpha, \alpha'$ -dithiol; C<sub>8</sub>H<sub>10</sub>S<sub>2</sub>) provides mechanical and electronic tethering of the Au cluster to the LTG:GaAs surface. The *I*(*V*) data of the Au cluster/xylyl dithiol/GaAs show ohmic contact behavior with good repeatability between various clusters distributed across the surface. The specific contact resistance is determined to be  $1 \times 10^{-6} \Omega \text{ cm}^2$ . Current densities above  $1 \times 10^6 \text{ A/cm}^2$  have been observed. © 1999 American Institute of Physics. [S0003-6951(99)02719-9]

There have recently been numerous examples of prototype electronic devices having nanometer-scale dimensions.<sup>1-4</sup> A requirement of many of these nanodevices is the presence of nearby contacts having dimensions of order 1  $\mu\text{m}$  or greater. Thus, even though the device has shrunk well into the nanometer scale, the contacts to the device still require areas  $\sim 10^2$ – $10^4$  greater than the active device. Nanocontacts having dimensions comparable to a nanodevice will be required to alleviate this difficulty in the future.

The demands on nanocontacts are quite stringent. In particular, suitable nanocontacts must provide low contact resistance and must be spatially uniform at the nanometer-length scale. This requirement presents significant problems for nanocontacts based on any alloying process. For instance, in compound semiconductor devices based on GaAs, conventional contacts such as alloyed Au/Ge/Ni on *n*-type layers are spatially nonuniform and also consume a significant surface layer.<sup>5</sup>

Low-temperature-grown GaAs (LTG:GaAs), i.e., GaAs grown at a temperature of 250–300 °C by molecular beam epitaxy, shows many interesting electronic properties that have been attributed to the  $\sim 1\%$ – $2\%$  excess arsenic incorporated during growth.<sup>6</sup> For as-grown material, the excess arsenic results in a high concentration ( $\sim 1.0 \times 10^{20} \text{ cm}^{-3}$ ) of point defects, primarily as arsenic antisite defects.<sup>6</sup> These

defects are observed as a band of states located in the GaAs gap. These states prevent the GaAs surface from rapidly oxidizing due to the relatively low concentration of minority-carrier holes in the surface layer.<sup>7,8</sup>

*Ex situ*, nonalloyed ohmic contacts employing a LTG:GaAs surface layer can provide specific contact resistivity ( $\rho_c$ ) below  $1 \times 10^{-6} \Omega \text{ cm}^2$ .<sup>9</sup> These contacts may be appropriate for nanometer-scale device applications since they would not suffer from the deep interface and spatial nonuniformity of Au/Ge/Ni contacts. Several device applications have been demonstrated for this contact,<sup>10</sup> but to date, to the best of our knowledge, the uniformity, performance and suitability as a nanocontact have not been discussed. These important issues are addressed in this letter.

The GaAs layer structure used in this study, shown in Fig. 1, employs a thin (10 nm) layer of LTG:GaAs to facilitate a high-quality, nanocontact to *n*<sup>+</sup> GaAs(100) layers grown at standard temperatures. To form a reliable electrical contact at the nanoscale, an organic monolayer of *p*-xylene- $\alpha, \alpha'$ -dithiol (C<sub>8</sub>H<sub>10</sub>S<sub>2</sub>), also denoted as xylyl dithiol (XYL), is used to tether a nanometer-size Au cluster to the LTG:GaAs layer. The lateral dimensions of the Au cluster thereby determine the size of the nanocontact. This structure can be used to contact active devices (to be incorporated at a later date) from above. *Ex situ* processing in a dry nitrogen atmosphere was used to deposit the XYL monolayer. The deposition involved soaking the sample in a 1 mM solution of XYL in acetonitrile for 12–18 h, followed by thorough rinsing in acetonitrile.

<sup>a)</sup>Permanent address: Motorola Inc., Austin, Texas 78721.

<sup>b)</sup>Electronic mail: rr@physics.purdue.edu

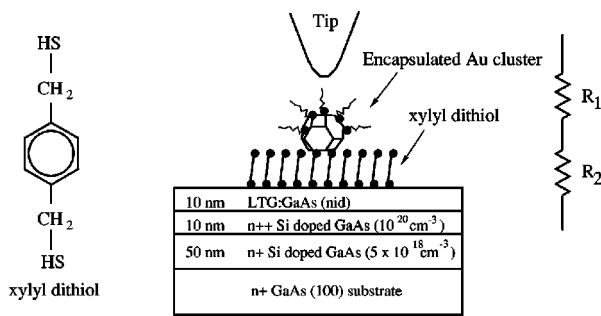


FIG. 1. A schematic diagram of the nanocontact structure showing the GaAs epitaxial layers, the xylyl dithiol monolayer (detail in inset), the deposited Au cluster encapsulated with dodecanethiol, and the STM tip.

Representative samples of the LTG:GaAs-capped and the XYL-coated layers were characterized using ellipsoscopy for surface imaging (EMSI),<sup>11</sup> an ellipsometric imaging technique with submonolayer sensitivity and a spatial resolution of  $\sim 3\mu\text{m}$ . EMSI can characterize the uniformity and stability of a thin (monolayer) coating as a function of position and time. The EMSI images on uncoated LTG:GaAs indicated that the optical properties (i.e., complex refractive index) varied with time, which can be attributed to a slow and uneven oxidation of the LTG:GaAs surface. The XYL-coated surface was observed to be uniform and stable, with no significant change in the EMSI images detected during several hours of exposure to atmosphere. This result suggests the presence of a uniform, monolayer coverage of XYL on the LTG:GaAs.

Controlled-geometry nanocontacts were formed on the coated LTG:GaAs by depositing dodecanethiol [ $\text{CH}_3(\text{CH}_2)_{11}\text{SH}$ ] encapsulated Au clusters having controlled mean diameters of  $\sim 4\text{ nm}$ . The single-crystal Au clusters were synthesized using a multiple expansion cluster source (MECS).<sup>12</sup> The random position of the Au clusters across the semiconductor surface allows assessment of the uniformity of the nanocontacts. In the resulting structure (Fig. 1), the XYL molecules provide both an effective mechanical tethering and a strong electronic coupling between the Au clusters and the LTG:GaAs surface. Since the XYL molecules have a thiol ( $-\text{SH}$ ) end group at each end, these molecules are ideal for forming a chemical bond to both the LTG:GaAs and to the faceted surfaces that are present on the Au clusters, the latter via a displacement reaction. The XYL molecules also serve as a molecular wire by establishing a conduction path from the Au cluster to the substrate.

An UHV STM was used to locate and probe the electronic properties of the nanocontacts. The same STM was also used to study the root-mean-square (rms) surface roughness of the as-grown LTG:GaAs and of the XYL-coated samples before depositing Au clusters. Representative values for the rms roughness over an area of  $100\text{ nm} \times 100\text{ nm}$  were  $\sim 0.4\text{ nm}$  for the as-grown LTG:GaAs and  $\sim 0.7\text{ nm}$  for the XYL-coated sample.

After depositing Au clusters, the stability of the nanocontacts were checked by performing 100 consecutive images over an 80 min period of time. From these measurements, the  $xy$ -drift rate was determined to be about  $0.9\text{ nm}/\text{min}$ . This should be compared to the time interval required to obtain a complete set of  $I(V)$  data, which is less than 1 s.

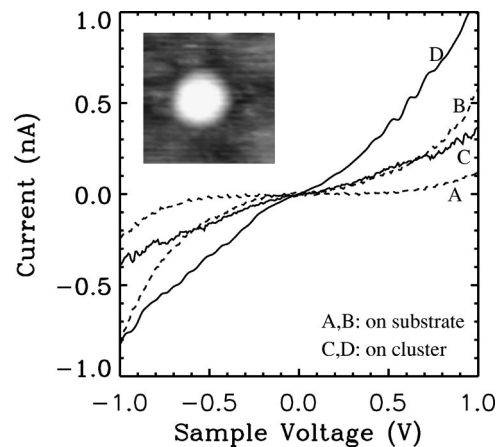


FIG. 2.  $I(V)$  data taken with the tip positioned over the XYL-coated substrate (dashed) and over the Au cluster (solid) with  $I_{\text{set}}=0.8\text{ nA}$  and  $-1.5\text{ V}$  [(A) and (C)],  $-1.0\text{ V}$  [(B) and (D)] for  $V_{\text{set}}$ . Inset picture is a  $25 \times 25\text{ nm}$  STM topographic image of Au cluster tethered to the XYL-coated LTG:GaAs, acquired with  $I_{\text{set}}=1.0\text{ nA}$  and  $V_{\text{set}}=-1.0\text{ V}$ . The apparent lateral dimension ( $13\text{ nm}$ ) is considerably broadened by tip convolution, but the height ( $3.4\text{ nm}$ ) is close to the diameter of the cluster.

The Au clusters were observed to remain stable and did not exhibit any damage. These observations indicate that the clusters are well tethered to the LTG:GaAs cap layer, in agreement with previous studies when Au clusters were tethered by XYL molecules to a flat gold substrate.<sup>13,14</sup>

The electronic properties of the Au nanocontacts were investigated by comparing a series of  $I(V)$ s obtained with the tip positioned over the Au cluster and over the XYL-coated LTG:GaAs substrate. Representative  $I(V)$  data are given in Fig. 2. When compared to the XYL-coated substrate, the nanocontact is found to exhibit an ohmic behavior, with a significant enhancement in the conduction for low bias voltages.

The ohmic behavior is found to persist to higher tunnel currents as shown in Fig. 3(a), which shows the  $I(V)$  behavior for a current up to  $30\text{ nA}$  when the tip is positioned over a Au cluster. In order to determine  $\rho_c$  and the maximum current capability, the current  $I$  was measured versus the tip-cluster spacing ( $z$ ),  $[I(z)]$ . As the tip contacts the cluster, the current is expected to saturate.<sup>15</sup> Figure 3(b) is a plot of  $I(z)$  obtained from the same Au cluster, with the tip moved by a total of  $1.5\text{ nm}$  from an initial height.

The Au cluster/XYL/GaAs system can be modeled by two resistors in series,  $R_1$  and  $R_2$ , where  $R_1$  represents the equivalent tunnel resistance between the STM tip and the Au cluster and  $R_2$  represents the equivalent contact resistance between the Au cluster and the GaAs substrate (see Fig. 1). Coulomb blockade effects, observed in earlier studies,<sup>13,14</sup> are not expected to occur here because of the relatively large size of the Au clusters employed. The data in Fig. 3(b) show that for a relative tip displacement of less than  $0.7\text{ nm}$ , the tunnel current increases exponentially with tip-cluster separation, indicating that  $R_1$  is dominant. As the separation between tip and cluster decreases, the current saturates and approaches an asymptotic value, indicated by the horizontal dashed line in Fig. 3(b). In this limit, the measured resistance is approximately equal to  $R_2$ .

The value of  $\rho_c=R_2 \times \mathcal{A}$  can be obtained using an estimate of the contact area  $\mathcal{A}$  between the Au cluster and sub-

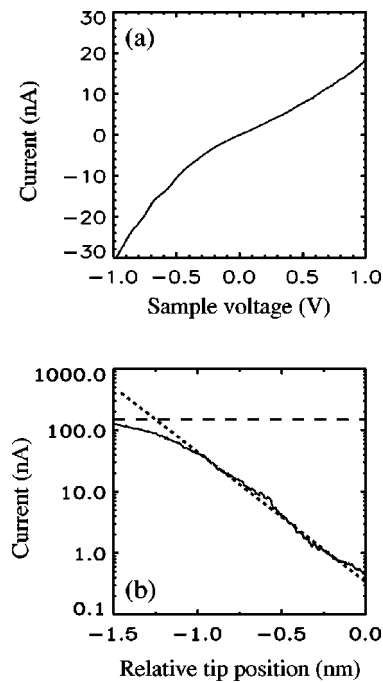


FIG. 3. (a)  $I(V)$  data from a Au cluster acquired with  $I_{\text{set}}=30$  nA and  $V_{\text{set}}=-1.0$  V. (b)  $\log(I)$  vs relative tip position above the same Au cluster, at constant  $V_{\text{set}}=-1.0$  V. The initial separation (plotted at zero) corresponds to  $I_{\text{set}}=0.5$  nA. The dotted line indicates an initial exponential dependence of  $I$  on  $z$  before current saturation occurs. The dashed line represents the estimated saturation current.

strate, which is available because of the well-characterized, single-crystalline Au clusters used in this study. From geometrical considerations, the area of a Au(111) facet on a  $\sim 4$  nm high, truncated octahedral cluster is  $\sim 9 \times 10^{-14}$  cm<sup>2</sup>. Using the asymptotic saturation current  $I_{\text{sat}} \approx 100$  nA at 1 V yields

$$\rho_c \approx (V/I_{\text{sat}})A \approx 1 \times 10^{-6} \Omega \text{ cm}^2. \quad (1)$$

This estimate assumes that the  $I(V)$  data are approximately linear for values of  $V$  up to 1 V, an assumption consistent with the data shown in Fig. 3(a). Although  $R_2$  includes contributions from the sheet resistance of the semiconductor layers and the relatively large-area clip on the top surface of the semiconductor, calculations indicate that it is dominated by two terms associated with current flow directly beneath the nanocluster. The first term is associated with electrons flowing from the electronic states of the Au cluster, through the XYL molecules, and into the midgap states in the LTG:GaAs layer. While a detailed prediction of the tunneling resistance for this system is not available, a resistance per molecule corresponding to a  $\rho_c$  in the range of  $10^{-7}$ – $10^{-6}$   $\Omega$  cm<sup>2</sup> has been predicted and experimentally verified for a Au/XYL/Au system.<sup>14,16</sup> The second term is a specific interlayer contact resistance  $\rho_{\text{int}}$  associated with the tunnel barrier between the LTG:GaAs layer and the underlying  $5 \times 10^{18}$  cm<sup>-3</sup> doped layer. We use the measured  $\rho_c$  from large-area contacts<sup>9</sup> ( $\sim 1 \times 10^{-6}$   $\Omega$  cm<sup>2</sup>) to provide an upper bound for  $\rho_{\text{int}}$ . The lateral transfer length for this current path  $l \approx \sqrt{\rho_{\text{int}}/R_{\text{shl}}}$ ,<sup>17</sup> is found to be a few nanometers for  $R_{\text{shl}} \approx 10^7$   $\Omega$  per square (the sheet resistance of the LTG:GaAs layer). Since the thickness of the LTG:GaAs layer is greater than the diameter of the nanocontact, it is expected that the current spreads

within the LTG:GaAs layer, and therefore, that the effective area for conduction into the  $n$ -doped layer is somewhat larger than the faceted area of the  $\sim 4$  nm Au clusters. Because of this current spreading, the value of  $R_2$ , and therefore the  $\rho_c$ , is expected to be dominated by the first of the two terms described here.

In conclusion, we have developed and characterized a nanometer-scale, ohmic contact to LTG:GaAs using molecular wire technology. Au clusters, deposited on the cap layer of LTG:GaAs, are found to be well tethered to the LTG:GaAs substrate by a monolayer of XYL molecules. The  $I(V)$  characteristics of the Au cluster/XYL/GaAs nanocontact exhibits an ohmic behavior with a specific contact resistance of  $\sim 1 \times 10^{-6}$   $\Omega$  cm<sup>2</sup>. This result compares favorably to reported values in the mid  $10^{-7}$   $\Omega$  cm<sup>2</sup> range obtained from studies using  $40 \mu\text{m} \times 100 \mu\text{m}$  contact pads.<sup>9</sup> Using this procedure, ohmic nanocontacts to buried active devices now seem feasible, especially if the Au cluster can be used as a self-aligned etch mask to delineate the structure of interest from the surrounding substrate, thereby allowing significant current to be channeled through it.

This work was partially supported by DARPA/Army Research Office under Grant No. DAAH04-96-1-0437, the NSF MRSEC program under Grant No. 9400415-G-0144, and AFOSR Grant No. F49620-96-1-0234A. The authors would like to thank S. Datta, C. P. Kubiak and J. Gomez for many helpful discussions throughout the course of this work.

- <sup>1</sup>D. L. Klein, R. Roth, A. K. L. Lim, A. P. Alivisatos, and P. L. McEuen, *Nature* (London) **389**, 699 (1997).
- <sup>2</sup>A. N. Korotkov, in *Molecular Electronics*, edited by J. Jortner and M. Ratner (Blackwell Science, Oxford, 1997).
- <sup>3</sup>D. Goldhaber-Gordon, H. Shtrikman, D. Mahalu, D. Abusch-Magder, U. Meirav, and M. A. Kastner, *Nature* (London) **391**, 156 (1998).
- <sup>4</sup>H.-L. Lee, S.-S. Park, D.-I. Park, S.-H. Hahm, and J.-H. Lee, *J. Vac. Sci. Technol. B* **16**, 762 (1998).
- <sup>5</sup>A. G. Baca, F. Ren, J. C. Zopler, R. D. Briggs, and S. J. Pearton, *Thin Solid Films* **308–309**, 599 (1997).
- <sup>6</sup>M. R. Melloch, J. M. Woodall, E. S. Harmon, N. Otsuka, F. H. Pollak, D. D. Nolte, R. M. Feenstra, and M. A. Lutz, *Annu. Rev. Mater. Sci.* **25**, 547 (1995).
- <sup>7</sup>S. Hong, D. B. Janes, D. McInturff, R. Reifenberger, and J. M. Woodall, *Appl. Phys. Lett.* **68**, 2258 (1996).
- <sup>8</sup>T. B. Ng, D. B. Janes, D. McInturff, and J. M. Woodall, *Appl. Phys. Lett.* **69**, 3551 (1996).
- <sup>9</sup>M. P. Patkar, T. P. Chin, J. M. Woodall, M. S. Lundstrom, and M. R. Melloch, *Appl. Phys. Lett.* **66**, 1412 (1995).
- <sup>10</sup>H. J. Ueng, V. R. Kolagunta, D. B. Janes, K. J. Webb, D. T. McInturff, and M. R. Melloch, *Appl. Phys. Lett.* **71**, 2496 (1997).
- <sup>11</sup>G. Haas, T. D. Pletcher, G. Bonilla, T. A. Jachimowski, H. H. Rotermund, and J. Lauterbach, *J. Vac. Sci. Technol. A* **16**, 1117 (1998).
- <sup>12</sup>S. P. Andres, J. D. Bielefeld, J. I. Henderson, D. B. Janes, V. R. Kolagunta, C. P. Kubiak, W. Mahoney, and R. G. Osifchin, *Science* **273**, 1690 (1996).
- <sup>13</sup>M. Dorogi, J. Gomez, R. Oschifin, R. P. Andres, and R. Reifenberger, *Phys. Rev. B* **52**, 9071 (1995).
- <sup>14</sup>R. P. Andres, T. Bein, M. Dorogi, S. Feng, J. I. Henderson, C. P. Kubiak, W. Mahoney, R. G. Osifchin, and R. Reifenberger, *Science* **272**, 1323 (1996).
- <sup>15</sup>N. D. Lang, *Phys. Rev. B* **36**, 8173 (1987).
- <sup>16</sup>M. P. Samanta, W. Tian, S. Datta, J. I. Henderson, and C. P. Kubiak, *Phys. Rev. B* **53**, 7626 (1996).
- <sup>17</sup>H. H. Berger, *Solid-State Electron.* **15**, 145 (1972).